PET Scanning and the Human Immunodeficiency Virus-Positive Patient

Michael J. O'Doherty, Sally F. Barrington, Meg Campbell, John Lowe and Caroline S. Bradbeer
The Clinical PET Centre, Genitourinary Medicine and Haemophilia Centre, Guys and St. Thomas Hospital Trust, St. Thomas' Hospital, London, United Kingdom

The use of PET scanning in patients with human immunodeficiency virus infection and fever of unknown origin, confusion and/or weight loss was investigated. **Methods:** Eighty patients were examined using PET. Fifty-seven patients had half-body scans with [^{18}F]fluorodeoxyglucose (FDG), and 23 patients had brain studies performed with FDG. Fourteen patients also had [^{11}C]methionine studies (2 chest, 1 abdomen and 11 brain) performed. **Results:** Thirteen patients with lymphoma had the extent of the disease clearly identified in both nodal and extranodal sites. Patients with a variety of infections (*Cryptococcus neoformans*, *Pseudomonas aeruginosa*, *Mycobacterium tuberculosis* and *Mycobacterium avium intracellulare*) had disease localized for appropriate biopsy or sampling procedures. A half-body FDG-PET scan had a sensitivity of 92% and a specificity of 94% for localization of focal pathology that needed treatment. High uptake of FDG (greater than liver) had a positive predictive value for pathology needing treatment of 95%. FDG brain studies showed that 16 patients with CD4 T-lymphocyte counts less than 200 cells/ml had reduced cortical uptake compared with that in basal ganglia. FDG scans were abnormal in all 19 patients with focal space occupying lesions identified by magnetic resonance scans. The standardized uptake values (SUVs) over cerebral lesions due to toxoplasma were in the range of 0.14–3.7 (13 patients) and due to lymphoma were in the range of 3.9–8.7 (6 patients). Three more patients with progressive multifocal leukoencephalopathy had SUVs in the range of 1.0–1.5 over the lesions. Another patient had a low-grade oligodendroglioma (SUV = 2.9). Carbon-11-methionine uptake also was high in patients with cerebral lymphoma but did not add to the discrimination between toxoplasmosis and lymphoma in these patients obtained with the FDG scan. **Conclusion:** In hospitals with access to PET facilities, FDG scanning allows the rapid evaluation of the whole body, including the brain, of patients with human immunodeficiency virus infection, with a report potentially available within 4 hr of injection. Sites of infection and tumor were identified, and discrimination between cerebral pathologies was possible.

Key Words: human immunodeficiency virus; PET; fluorodeoxyglucose; methionine; infection; tumor

J Nucl Med 1997; 38:1575–1583

Patients with human immunodeficiency virus (HIV) infection are at risk of developing a variety of infections and tumors that may generate a fever, without any localizing features, or nonspecific weight loss, which may lead to classification of the individual as having acquired immunodeficiency syndrome (AIDS) (*1–3*). Accompanying these fevers, there may be decompensation of mental function or disorientation, which may or may not be related to focal cerebral pathology. The patients may have multiple pathologies, with combinations of infection and tumor leading to their problems. Often the causes of fever, disorientation and weight loss are readily found upon clinical examination, a chest radiograph, blood cultures and routine biochemical or hematologic analyses. However, imaging is necessary in many cases to direct the clinician to the probable source of the patients' symptoms. This direction has routinely been provided by ^{67}Ga scanning, particularly if there are no definite localizing features or the thorax is thought to be the most likely site for symptoms (*4–6*). There are pitfalls, however, of using this tracer. Physiological secretion of gallium in the bowel makes evaluation of the abdomen difficult (*7–9*). The brain is not well-visualized, and the appearances of persistent generalized lymphadenopathy (PGL) and lymphoma may be similar. The time taken to complete a study, 24–72 hr, also represents a considerable disadvantage.

Fluorine-18-fluorodeoxyglucose (FDG) PET scanning is now widely used in the evaluation of patients with tumors (*10*) and, in particular, has been used in the staging of patients with lymphoma (*11*). The use of FDG in the brain has included defining the grade of tumors (*12,13*) and, in patients with HIV infection, has allowed the distinction between patients who have cerebral toxoplasmosis and cerebral lymphoma (*14*). The extent of cerebral tumors has been better defined using [^{11}C]methionine (MET) (*15*), and there has been demonstrable uptake in a patient with a cerebral abscess (*16*). It is possible that the combination of FDG and MET may further define cerebral lesions in HIV.

The purpose of this study was to evaluate the possible use of FDG-PET scanning in HIV-positive patients, in particular, the distribution in patients with PGL and in those patients with fever and weight loss, with or without cerebral pathology. The ability of MET to improve the diagnostic yield in cerebral imaging was also assessed.

MATERIALS AND METHODS

All HIV-positive patients with a fever and/or confusion or weight loss, who had no clinical evidence (clinical history, examination, chest radiograph or oxygen saturation) of *Pneumocystis carinii pneumonia*, were studied with a FDG half-body PET scan. Half-body FDG scans were requested in patients who had a fever, and the question of lymphoma or focal infection was included in the differential diagnosis. If a space-occupying abnormality was identified on magnetic resonance (MR), a combination study of MET and FDG was requested to assess whether a cerebral tumor was present rather than another cause. Localized, attenuation-corrected views of the chest or abdomen were also acquired where possible, if focal pathology was suggested by symptoms, clinical examination or other imaging so that semiquantitative information in the form of standardized uptake values (SUVs) could be obtained over areas of interest. When cerebral pathology was suspected either from clinical findings or an initial MR scan, brain imaging with both MET and FDG was performed. All patients referred for PET scans were initially started on standard therapy for toxoplasmosis. The scans were performed within 5 days of admis-

Received Jul. 25, 1996; revision accepted Dec. 19, 1996.
For correspondence or reprints contact: Michael J. O'Doherty, MD, FRCP, The Clinical PET Centre, Guys and St. Thomas Hospital Trust, St. Thomas' Hospital, London SE1 7EH, United Kingdom.

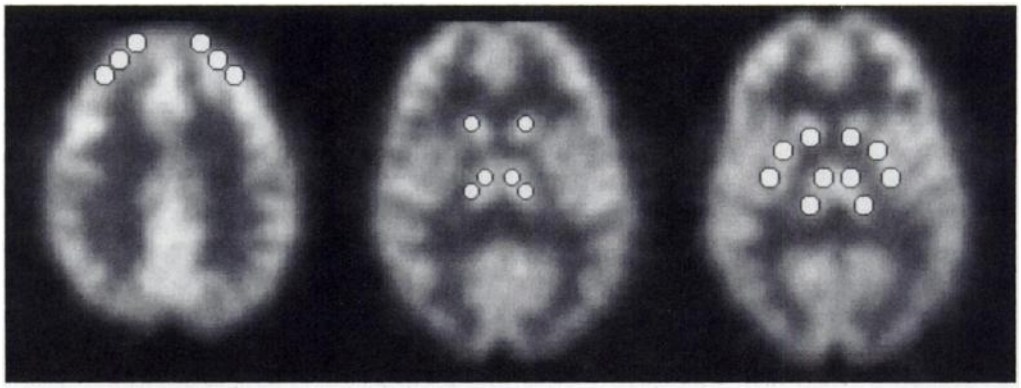

FIGURE 1. ROI template indicating the 22 ROIs that were placed on summed planes and averaged to obtain regional count ratios.

sion and within 5 days of an MR scan. All patients were followed for a median period of 9 mo or until death.

Fluorine-18-fluoride was produced in a cyclotron by proton bombardment of a high-pressure water target. FDG was synthesized by nucleophilic substitution of a precursor by $^{18}F^-$. S-Methyl-MET is an amino acid produced from the reaction of the precursor, L-homocysteine thiolactone, with [^{11}C]methyliodide (*17,18*). Carbon-11-methyliodide is produced from ^{11}C-carbon dioxide using a fully automated system, "Synthia," designed and built at Uppsala University PET center (*17*).

All PET scans were performed after a 6-hr fast using a whole-body scanner. The scan protocols were as follows.

Cerebral Studies

Patients with known ring-enhancing lesions or areas suggestive of progressive multifocal leukoencephalopathy on MR scanning were scanned with FDG and MET. All patients were treated for between 3 and 5 days with antitoxoplasma therapy (sulfadiazine and pyrimethamine) before scanning. Patients who were compliant and not confused had a FDG brain study in addition to the whole-body scan. Patients were positioned supine within the field of view of the camera and injected intravenously with 370 MBq of [^{11}C]MET, with scan images from skull base to vertex acquired 15 min postinjection. Thirty-five minutes after the initial injection, i.e., immediately after the acquisition of the MET, 250 MBq of [^{18}F]FDG was injected (with the patient in a quiet rested state), and imaging was repeated using external markers and a head restraint to ensure identical positioning of the patient for both scans. In some patients, sequential imaging with the two tracers was not possible, and an initial 2-min "test" emission scan was used to match the alignment of the patient's head to that of the earlier scanning session. Thirty-one contiguous slices were produced over a 10.8-cm axial field of view with four (MET) or six (FDG) sequential static scans of 5-min duration each acquired (the duration of the MET scan is optimal to balance uptake of tracer against loss of counts due to the decay of the tracer). Frames were then summed to produce high-quality images, with those frames showing excessive movement rejected. Each slice thickness was 3.5 mm. Calculated attenuation correction was performed (*19*); this saved time for the patient study and has been demonstrated to be a reliable method in the brain. The complete set of image planes was reconstructed and smoothed to obtain two image datasets, one for each tracer, with a spatial resolution of 8 mm in all three orthogonal directions. Methionine and FDG brain images were displayed adjacently and viewed simultaneously slice by slice in coronal, transaxial and sagittal planes. A visual report was provided by two experienced nuclear physicians with access to the clinical information and other imaging results. SUVs were obtained by placing 8-mm circular regions of interest (ROIs) over areas of maximal or minimal uptake within individual "hot" or "cold" cerebral lesions, identified by the two clinicians, and the average activity per ml in the ROI was obtained with a knowledge of a calibration factor obtained by scanning a uniform 20-cm cylinder containing a known activity concentration. This value was then normalized for body weight and injected activity. A partial volume correction was applied to lesions measuring less than 2 cm diameter on the image (*20*). The partial volume correction factors were obtained from a phantom study of a series of cylinders ranging in diameter from 8 to 40 mm. Lesion-to-contralateral brain ratios were also obtained with one or the mean of several 8-mm circular ROIs placed individually over the lesions and corresponding contralateral areas within the brain, using the MR scans to indicate the site of space-occupying lesions.

A template (Fig. 1) was used to place 7-mm circular ROIs over fixed sites in the frontal cortex, thalami and basal ganglia in a group of 16 patients who had no focal pathology in the brain and no specific abnormality on the half-body study or long-term follow-up (12 mo). The ratio between the frontal cortex and the thalami and basal ganglia was used to examine the distribution of FDG in these areas of the brain.

Effective dose equivalent for 250 MBq [^{18}F]FDG is 6.8 mSv, and for 350 MBq of [^{11}C]MET, it is 1.7 mSv.

Half-Body Studies

The patients were injected with 350 MBq [^{18}F]FDG and imaged 45–60 min later with half-body images obtained by acquiring 10 consecutive 5-min images from the vertex of the skull to the midthigh, unless a separate cerebral study was performed, in which the patient was scanned from the neck to midthigh. (In cases for which cerebral and half-body studies were both required, they were done in the same scanning session, with a single FDG injection and with the brain study performed first.) The complete sets of 310 image planes were reconstructed and smoothed in the axial direction to obtain a single three-dimensional dataset with a spatial resolution of 10 mm. Images were viewed as a projection image and on a slice-by-slice basis as transaxial, coronal and sagittal volume images. In some patients, single or two adjacent local emission scans lasting 15 min each were also obtained over an axial field of view, measuring 10.8 cm. Either corresponding transmission images were acquired at the commencement of the scanning session, or simultaneous transmission/emission images were acquired on completion, using rotating ^{68}Ge rod sources to allow for attenuation correction during image reconstruction. The spatial resolution of these reconstructed localized "emission/transmission" volume images was 13 mm in all three planes. A visual report was again provided by two experienced nuclear physicians, with access to the clinical information and other imaging results. The uptake within focal lesions was graded as high, moderate or low using the liver as the reference organ. Therefore, high uptake was greater than liver uptake, moderate was equal to liver uptake and low was less than liver uptake but greater than background.

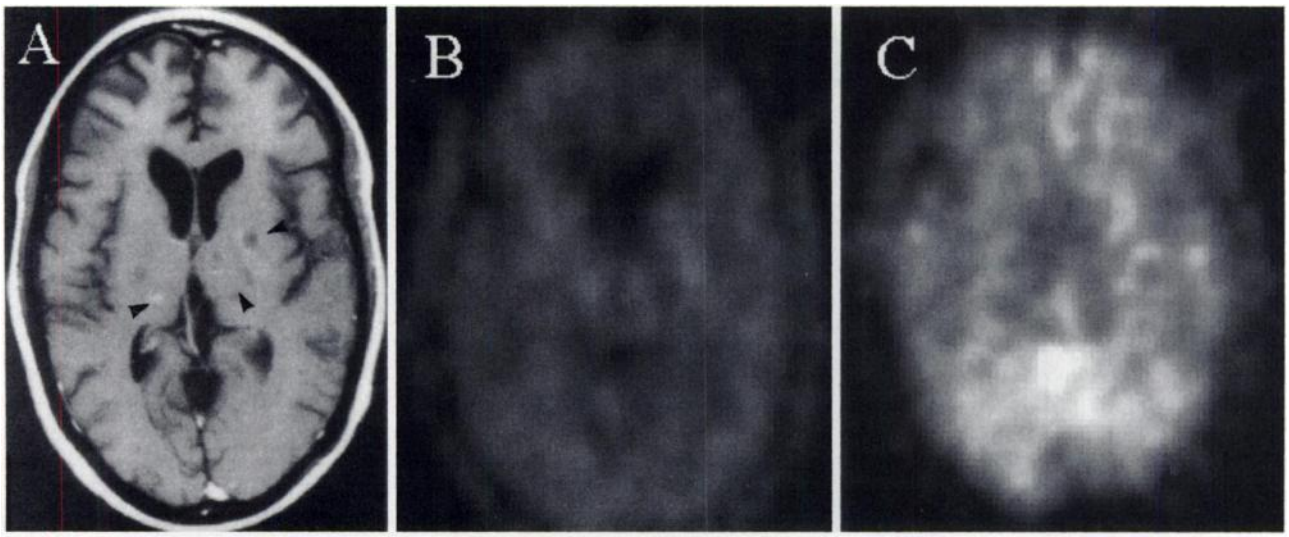

FIGURE 2. MR appearances in a patient with cerebral toxoplasmosis (indicated by arrowheads) (A), demonstrating the low-grade uptake of FDG (B) and MET (C) within the lesions, indistinguishable from adjacent normal brain tissue.

SUVs were obtained using 8-mm circular ROIs over any lesions visible on local views.

Follow-up scans were performed in patients treated for lymphoma (one patient) or if patients had a negative scan and presented at a later date with new symptoms of fever and weight loss (nine patients).

Effective dose equivalent for 350 MBq [^{18}F]FDG is 9.6 mSv.

Statistical comparison was performed using the two-tailed paired Student's t-test for the intracerebral SUV comparison of the space-occupying lesions and a Student's t-test for the comparison of the basal ganglia- and thalamic-to-cortical ratios.

RESULTS

Eighty patients (72 men and eight women), mean age 29.6 yr (range, 17–53 yr), were referred for clinical studies in which a total of 90 scans were performed. This included 23 patients with cerebral space-occupying lesions, of whom all had FDG scans, and 11 had scans with MET in addition. Fifty-seven patients had fever with no definite localization of disease and had half-body FDG studies. Ten patients underwent more than one study, and 16 of the 57 patients had both cerebral localized views and half-body studies. All patients had CD4 T-lymphocyte counts of less than 300 cells/mm^3, with 90% of patients having less than 150 cells/mm^3 (range, 10–300 cells/cmm).

Cerebral Studies

Thirteen patients were diagnosed as having cerebral toxoplasmosis by complete response to treatment or at autopsy. Figure 2 demonstrates the low-grade uptake seen with toxoplasmosis. The SUVs are demonstrated in Table 1. The difference between the lesion and contralateral normal brain is significant ($p < 0.00001$). The variability in the SUVs in "normal" brain is accounted for by the fact that space-occupying lesions have involved part of the basal ganglia, which results in high uptake in the contralateral brain because the ROIs are drawn over these structures. The SUVs over cerebral lesions due to toxoplasma were in the range of 0.14–3.7.

Six patients with lymphoma were diagnosed by biopsy or autopsy. The SUV measured over the lesions is shown in Table 1. The difference between the lesion and normal brain is significant ($p < 0.00001$). An example of multiple areas of increased uptake of both FDG and MET are shown in Figure 3. Three patients with PML diagnosed by clinical behavior and MR imaging (MRI) scan appearances showed normal uptake. The MR scan and FDG- and MET-PET scans are demonstrated in Figure 4. The SUVs over cerebral lesions due to lymphoma were in the range of 3.9–8.7.

The cerebral scan with FDG showed a sensitivity and specificity of 100% for identifying lymphoma, with a SUV range of 3.9–8.7 for FDG. The absence of increased uptake over an identified ring-enhancing lesion was found in all patients with cerebral toxoplasmosis.

Sixteen patients had FDG studies and were classed as having no definite cognitive dysfunction. The mean ratio ± s.d. between frontal cortical uptake of FDG and basal ganglia uptake on the left and the right were 0.81 ± 0.13 and 0.79 ± 0.12, respectively, and for the cortical-to-thalamic ratio, they were 0.95 ± 0.15 and 0.99 ± 0.14. The difference between the cortex-to-thalamic and the cortex-to-basal ganglia ratios was significantly different ($p = 0.002$). An example of one patient is shown in Figure 5.

Half-Body FDG Studies

The number of patients studied was 57. The pathologies found in 29 patients are shown in Table 2. Fifteen patients were known to have PGL, and the uptake in these nodes varied, as shown in Figure 6. Discrete uptake in the lymphadenopathy was shown to be present in four of the 15 patients; none of these patients developed an identifiable disease process within 6 mo of the scan. The majority, therefore, had no or very low-grade uptake by visual inspection. Seventeen patients had no identifiable abnormalities on the half-body PET scans; of this group, no cause for the pyrexia was found in 11 patients, and the temperatures settled without definitive treatment. Three had cytomegalovirus (CMV) infection (retinal) and were already receiving ganciclovir treatment intravenously, one had a cardiomyopathy with no infective cause found, and two had cryptococcal meningitis.

Three patients had Kaposi's sarcoma, two with parenchymal lung lesions identifiable on the chest radiograph. The FDG and MET uptakes were moderate grade in one patient (Fig. 7) and low grade in two patients, with patchy distribution throughout both lung fields. No uptake was identified in lymph nodes.

Thirteen patients were identified as having lymphoma. The uptake was identified in both soft tissue, lymph nodes and bone. The FDG uptake improved in the one case who had a follow-up scan after treatment with chemotherapy (Fig. 8). The B-cell lymphomas were all of a high grade. Patients with T-cell lymphoma were identified (Fig. 9).

TABLE 1
FDG and MET Brain SUVs Located over Lesions and the Contralateral Hemisphere at a Similar Position

Patient no.	Condition	Proof	SUV (FDG) lesion	SUV (FDG) contra	SUV (MET) lesion	SUV (MET) contra
1	Toxo	Treatment response	2.3	4.4		
2	Toxo	Treatment response	2.2	3.8		
			1.8	4.0		
			2.6	3.5		
3	Toxo	Treatment response	3.7	5.6	1.4	0.6
4	Toxo	Treatment response	1.8	3.6		
5	Toxo	Treatment response	2.0	3.0	0.8	1.0
			2.3	2.9	1.0	1.0
6	Toxo	Autopsy	2.0	3.0		
7	Toxo	Treatment response	1.7	4.2		
			1.1	4.0		
			1.9	4.4		
8	Toxo	Treatment response	2.4	3.6	1.1	1.2
			2.2	3.0	0.8	1.1
9	Toxo	Treatment response	0.1	1.0	0.1	0.4
			0.2	1.0	0.1	0.7
			0.2	1.0	0.1	0.7
10	Toxo	Treatment response	1.1	1.5		
11	Toxo	Treatment response	1.4	1.7		
12	Toxo	Treatment response	2.6	2.7		
13	Toxo	Treatment response	2.2	3.7	1.0	1.0
14	NHL	Brain biopsy	7.6	4.1		
15	NHL	Brain biopsy	4.9	1.6	1.0	0.5
			4.2	2.3	0.4	0.4
16	NHL	Autopsy	5.5	3.8	0.6	0.6
			4.9	2.4	0.5	0.3
17	NHL	Autopsy	5.5	2.4	4.7	0.8
			3.9	2.9	0.9	0.7
18	NHL	Autopsy	8.7	4.0		
			6.1	4.0		
19	NHL	Autopsy	6.8	2.9		
20	oligo	Autopsy	2.9	3.0	0.9	0.5
21	PML	MRI appearance and clinical	1.5	1.8	0.2	0.4
			1.0	1.4	0.5	0.6
22	PML	MRI appearance and clinical	1.0	1.3	0.2	0.3
23	PML	MRI appearance and clinical	1.5	1.7		

Where there was more than a single lesion, SUV analysis was performed over each identifiable individual lesion. Toxo = toxoplasmosis; NHL = nonhodgkins lymphoma; PML = progressive multifocal leucoencephalopathy; Oligo = oligodendroglioma.

Nine patients were identified as having soft tissue infection, leading to sampling (biopsy, aspiration or sputum collection) of the relevant sites. Two had *Pseudomonas* infection of the lung (Fig. 10), three had *Mycobacterium avium intracellulare* infection of lymph nodes, one had *Mycobacterium tuberculosis* infection (Fig. 11) and two had cryptococcal infection of the lungs with mediastinal nodal uptake. A further patient had staphylococcal infection of the right kidney (Fig. 12).

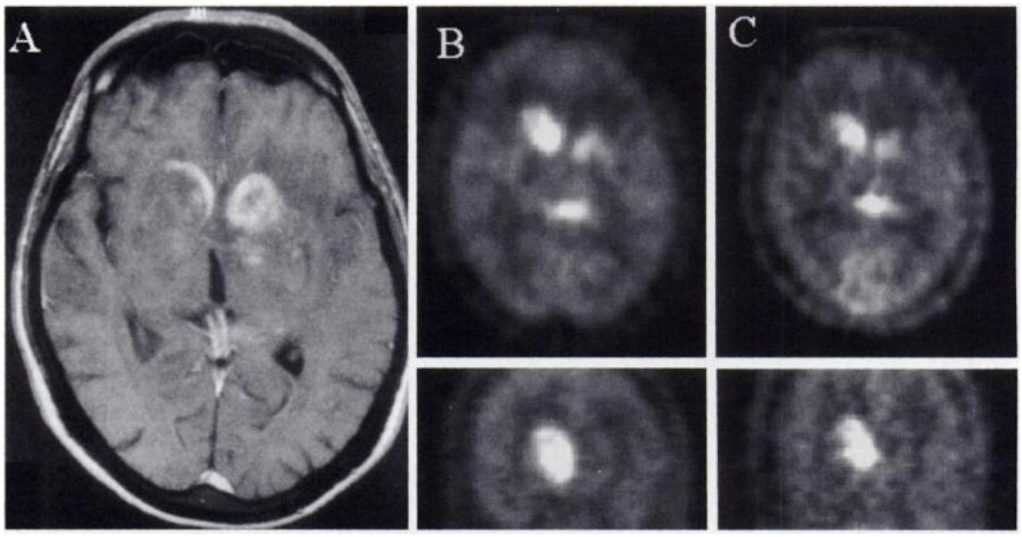

FIGURE 3. MR appearances in a patient with cerebral lymphoma (A), demonstrating the high-grade uptake of both FDG (B) and MET (C) within the lesions, shown in transaxial and coronal slices.

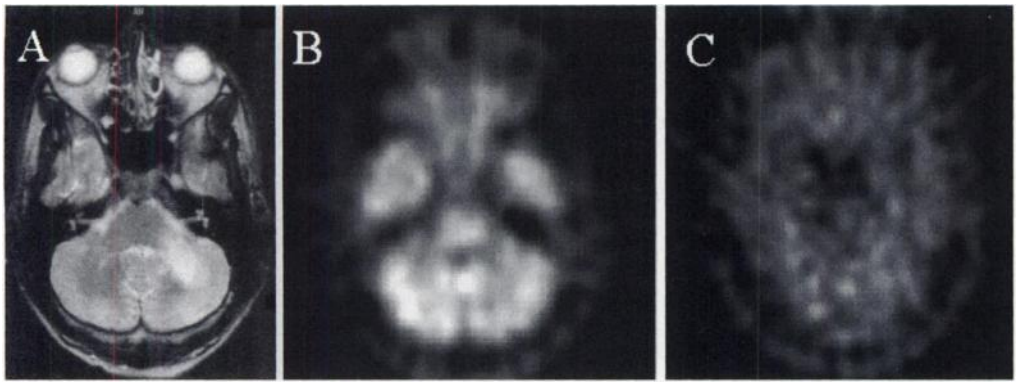

FIGURE 4. MR appearances in a patient with progressive multifocal leukoencephalopathy showing abnormal signal in the left cerebellum (A), demonstrating the low-grade uptake of FDG (B) and MET (C) within the lesion.

Ten patients had repeat studies. One patient with lymphoma demonstrated resolution of the disease. One patient had a repeat study after the initiation of treatment for *Mycobacterium avium intracellulare* infection and showed reduction in FDG uptake in the mesenteric lymph nodes where the initial infection was identified. Another patient showed resolution of the *Pseudomonas* infection in the chest and no new disease. The remaining seven patients demonstrated no change from the previous scan, and no focal pathology was identified on follow-up.

The half-body FDG study in 57 patients identified 20 patients with focal areas of high uptake (defined as uptake greater than liver uptake). There was one false-positive patient (PGL confirmed by biopsy). Nineteen patients had disease (either lymphoma or infection) identified by biopsy. The positive predictive value for a high-uptake scan for identifying a pathological abnormality needing treatment is 19 of 20, or 95%.

Moderate uptake on the scan (defined as equivalent to liver uptake) was present in five patients, one with pulmonary Kaposi's sarcoma, one with PGL, one patient with a T-cell lymphoma in the esophagus and buccal cavity and two patients with cryptococcal infection of the lung. Four patients had low uptake, two patients with PGL and two patients with pulmonary Kaposi's sarcoma.

Twenty-eight patients had no demonstrable uptake in lymph nodes or soft tissue on a half-body scan. None of these patients had further disease identified other than the disease known to be present at the time of the scan [CMV retinitis; cryptococcal meningitis in two patients; one patient with cardiomyopathy (HIV-related)].

The overall sensitivity for a positive test with moderate to high uptake was 23 of 25, or 92%; overall specificity was 30 of 32, or 94%, indicating pathology needing therapy.

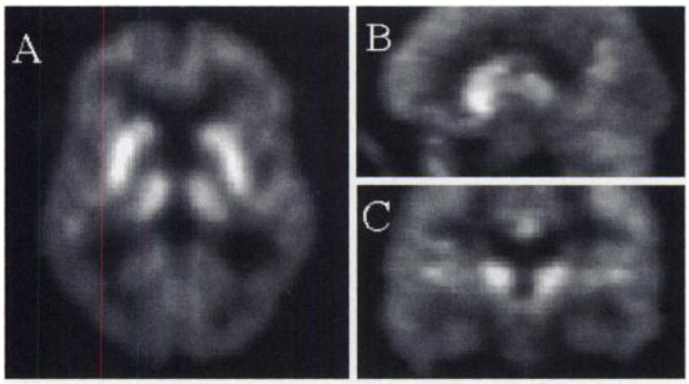

FIGURE 5. Uptake pattern of FDG seen within the brain of an HIV patient with no cognitive defect nor focal cerebral pathology. Transaxial (A), sagittal (B) and coronal (C) slices are shown. High uptake within the basal ganglia and thalami and increased separation of the thalami are seen; this was the common finding in the 16 patients with no cognitive dysfunction.

DISCUSSION

Immunosuppressed patients present a major challenge to the investigator because the disease process may result in a variety of opportunistic infections or tumors contributing to the cause of fever. The most common cause of fever of uncertain origin, however, is infection and is normally found in 82% of persons (*21*). The difficulty is in choosing the relevant site to biopsy or in having the confidence to treat empirically. The use of rapid imaging methods should aid the patient in terms of reducing the time to the initiation of definitive treatment or for biopsy to be performed.

Gallium-67 scanning has long been used to investigate patients with a fever, with certain obvious advantages. The scan allows assessment of soft tissue and bone abnormalities with a high sensitivity (*6*) and a very high sensitivity in the lung, especially when the chest radiograph is normal (*22*). The problem is that scanning often has to be delayed because gallium is not necessarily available "on the shelf" and interpretation usually takes 24–72 hr from the time of injection. There are also difficulties with imaging the abdomen because of gallium secreted into the bowel. With regard to the assessment of the lung parenchyma for *Pneumocystis carinii* pneumonia, a rapid method has been described using ^{99m}Tc diethylene triamine pentaacetic acid (DTPA) (*23*), which has been shown to have a higher sensitivity than gallium (*24*). Thus, the combination of a DTPA scan with an FDG-PET scan would allow a whole-body assessment of disease, theoretically on the day of admission or even as an outpatient procedure. There would also be a major reduction in radiation dose to the patient using this approach because the effective dose equivalent for a gallium scan, with administration of 150 MBq, is 18 mSv, compared with that for a FDG study of 9.6 mSv. The expansion of PET into the clinical arena has meant that several centers could offer this technique to study patients with HIV. The problem to be addressed is the range of abnormalities visualized with PET and whether HIV patients present unusual problems for PET imaging.

This preliminary data on FDG-PET scanning in patients with HIV and fever, confusion or weight loss is encouraging, showing an overall sensitivity of 92%, if moderate- and high-grade uptake are seen, and a specificity of 94%. Some of the same pitfalls that have been reported with gallium scanning are, however, also seen with FDG. Variable uptake of FDG was observed in the lymph nodes of patients who had PGL, as illustrated in Figure 6. Of 15 patients, high uptake was only observed in 1 patient; 3 had low-grade uptake and 11 patients with PGL had no uptake. The degree of uptake observed by visual analysis can, therefore, only give a likelihood as to whether there is tumor present. SUV analysis using simultaneous emission and transmission measurements for attenuation

TABLE 2
Half-Body FDG Results in HIV-Positive Patients with Fever and High, Moderate or Low Uptake of FDG

Patient no.	Visual score of uptake	Site of uptake	Disease diagnosis
1	High	Lymph nodes	T-cell lymphoma
2	High	Lymph nodes	T-cell lymphoma
3	High	Lymph nodes	B-cell lymphoma
4	High	Lymph nodes	B-cell lymphoma
5	High	Lymph nodes + right sacroiliac joint + abdominal skin	B-cell lymphoma
6	High	Breast + abdominal lymph nodes	T-cell lymphoma
7	High	Lymph nodes	B-cell lymphoma
8	High	Lymph nodes	B-cell lymphoma
9	Moderate	Oropharynx + esophagus	T-cell lymphoma
10	High	Lymph nodes	B-cell lymphoma
11	High	Unilateral sinus uptake	B-cell lymphoma
12	High	Lymph nodes + right lung	B-cell lymphoma
13	High	Gastric	B-cell lymphoma
14	High	Lymph nodes	MAI
15	High	Lymph nodes	*M. tuberculosis*
16	High	Lymph nodes	MAI
17	High	Lymph nodes	MAI
18	Moderate	Lymph nodes	*Cryptococcus* pulmonary infection
19	Moderate	Lymph nodes	*Cryptococcus* pulmonary infection
20	High	Right kidney	*Staphylococcus aureus* pyonephrosis
21	High	Right lung	*P. aeruginosa* pneumonia
22	High	Right lung	*P. aeruginosa* pneumonia
23	Moderate	Both lungs	Kaposi sarcoma
24	Low	Both lungs	Kaposi sarcoma
25	Low	Both lungs	Kaposi sarcoma
26	High	Lymph nodes	PGL
27	Moderate	Lymph nodes	PGL
28	Low	Lymph nodes	PGL
29	Low	Lymph nodes	PGL

MAI = Mycobacterium avium intracellulare.

correction of whole-body PET described by Meikle et al. (*25*) may allow the discrimination between PGL and other pathology or local transmission/emission scans performed over areas of known lymphadenopathy. This was not routinely performed in this study. Why increased uptake was observed in this proportion of patients is difficult to say. It is possible this is a reflection of the turnover of lymphocytes at this particular time because patients with PGL do experience intermittent enlargement of their lymph nodes that is detectable on a gross scale; this may occur on a less dramatic scale and cause uptake of FDG.

The FDG scans successfully localized tumor in patients with non-Hodgkin's lymphoma in soft tissue, in nodal and osseous sites and in the patient illustrated who underwent chemotherapy; the progress of disease could be followed, as has been documented in tumors in non-HIV-positive patients (*26–29*). The scan also allowed visualization of T-cell lymphoma (Fig. 9) localized in the oropharynx and the distal part of the esophagus, although the uptake of FDG in the esophagus was low grade. We believe, however, that esophagitis of other cause, i.e., *Candida* or CMV, may be visualized with the same low-grade intensity, and therefore the FDG will only point to an area that needs further study.

FDG-PET scanning, although thought to act mainly as a tumor-imaging agent in half-body scans, has been shown to be a nonspecific tracer, and as such, it should localize infective abnormalities (*30*). Infections in lymph nodes and soft tissue may be demonstrated as part of an evaluation. In this study, a

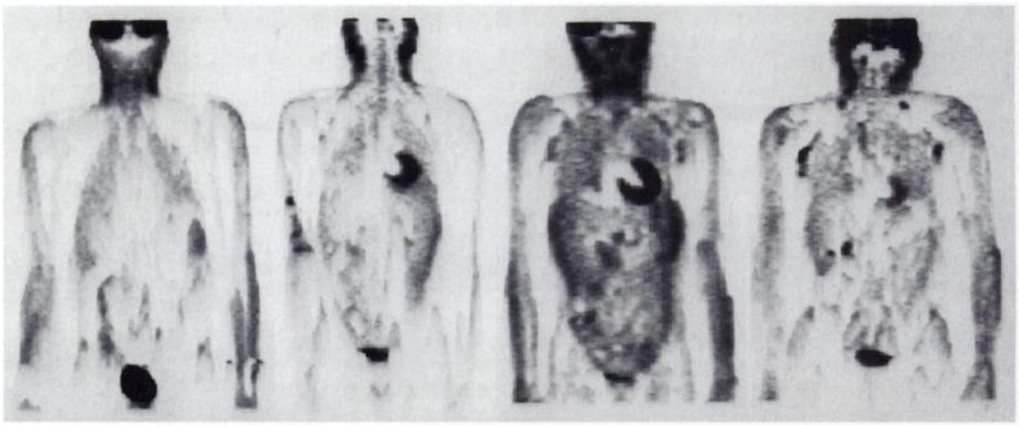

FIGURE 6. Variable uptake of FDG in lymph nodes of four of the 15 patients with PGL.

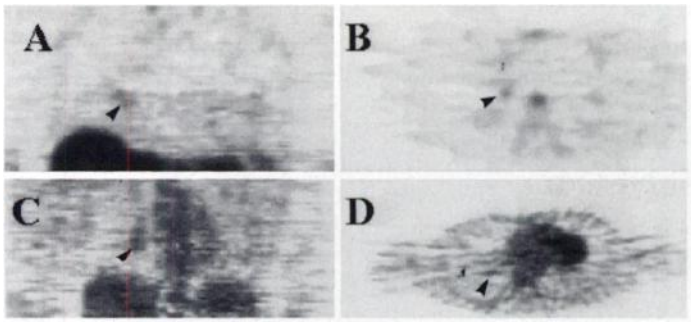

FIGURE 7. Low-grade uptake of MET (A and B) and FDG (C and D) (indicated by the arrowheads) in the lung fields of patients with Kaposi's sarcoma.

variety of infections have been demonstrated. Uptake in lymph nodes were seen with cryptococcal infection as well as mycobacterial infection. The intensity of uptake visually was such that separation from malignancy was not possible. Soft tissue and pulmonary infections were also visualized as an unexpected finding in three of the 80 patients scanned as part of assessment for other disease processes, i.e., lymphoma or mycobacterial infection and before the development of chest radiograph abnormalities. Infections identified included the localization of *Streptococcus pneumoniae* pneumonia and *Pseudomonas aeruginosa* and mycobacterial infection. A pyonephrosis was also demonstrated, allowing specific drainage to be performed. If high-grade uptake of FDG is used to define abnormality, then the positive predictive value for disease at this site is 95% and is useful clinically to direct biopsy to that site. A negative scan is also extremely useful in that focal infection or tumor is excluded. The presence of Kaposi's sarcoma in lymph nodes or soft tissue outside the lungs may pose a problem because our study did not include this group of patients.

The place of FDG in the assessment of cerebral infection, inflammation and malignancy has been suggested by Hoffman et al. (*14*). As many as 10% of patients with AIDS present with neurological symptoms, and up to 40% will develop neurological sequelae during the course of the illness (*31*). HIV is neurotrophic and may cause an encephalopathy and progressive dementia, with up to 87% of patients at autopsy having demonstrable neurological involvement (*32,33*). In addition, the brain may be affected by both opportunistic infections and malignancy.

Toxoplasma gondii is the most common treatable opportunistic infection that affects the central nervous system (CNS), but it may be difficult to distinguish from cerebral lymphoma; CT and MRI abnormalities are very similar (*34*), and in 95% of cases, CNS toxoplasmosis represents a reactivation of previous infection with little or no change in serological variables. It has been suggested that patients with cerebral mass lesions should receive empirical antitoxoplasma therapy (pyrimethamine and sulfadiazine) and that, if there is no response after 2 wk, then cerebral biopsy should be considered. Empirical therapy is, however, not without morbidity, and adverse effects are frequent. Many patients with AIDS will be receiving other drugs, thus increasing the risk of adverse reactions. Cerebral biopsy is invasive and carries a significant risk in immunocompromised patients, particularly if there is a bleeding diathesis. Thus, a noninvasive diagnostic test for the assessment of cerebral mass lesions in AIDS may be able to select those patients for biopsy and those for empirical therapy.

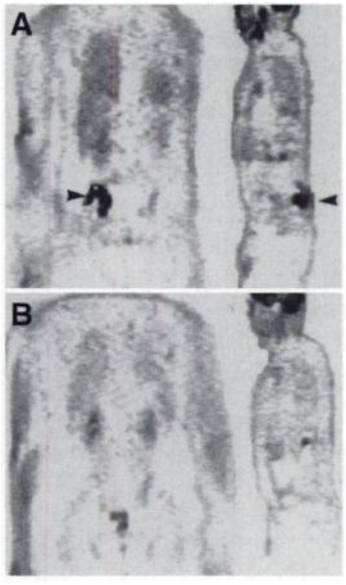

FIGURE 8. A patient with marked increased uptake of FDG in the right sacroiliac joint due to non-Hodgkin's lymphoma (indicated by arrowheads) immediately before treatment (A) and after treatment with chemotherapy (B).

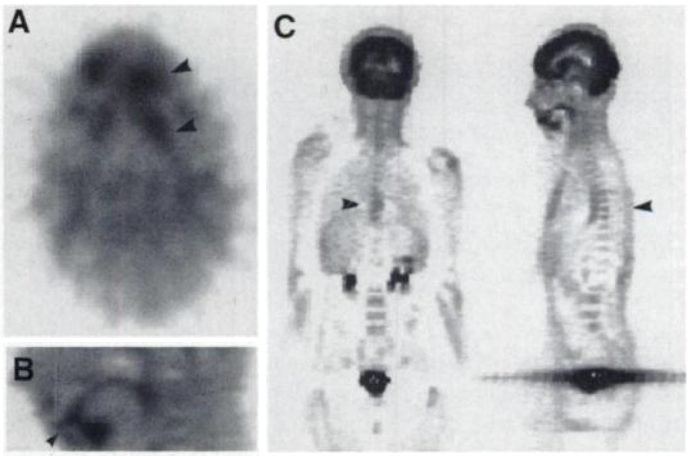

FIGURE 9. Uptake of FDG in a patient with a T-cell lymphoma of mouth [local transaxial (A) and sagittal (B) views, indicated by the arrowheads] and the esophagus (indicated by the arrowheads) illustrated on the whole-body coronal and sagittal images (C).

An increased accumulation of FDG has been demonstrated in cerebral lymphoma (*35*). Hoffman et al. (*14*) have recently suggested that FDG-PET imaging may have a potential role in differentiating lymphoma from infective CNS lesions, and similar results were found by Villringer et al. (*36*) in 11 patients studied with cerebral space-occupying lesions in patients with AIDS. MET-PET has been shown to be useful in defining the extent of cerebral gliomas (*15*), and it provides information additional to that of FDG-PET. In a single case report, a brain abscess accumulated MET (*16*), and therefore it was thought that a ratio between FDG and MET accumulation might improve the discrimination between malignant and nonmalignant disease. Our own study demonstrates that there is substantially higher uptake of both FDG and MET in lymphoma than in toxoplasmosis. This result, however, is in the context of

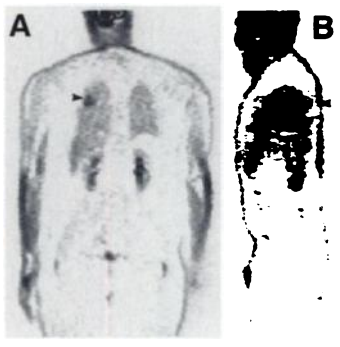

FIGURE 10. Uptake of FDG in a patient who developed a *P. aeruginosa* infection of the right lung (indicated by the arrowheads), coronal (A) and sagittal (B) images.

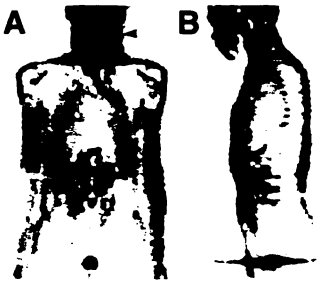

FIGURE 11. Multiple sites of FDG uptake (cervical, supraclavicular, mediastinal, paraaortic and mesenteric lymph nodes) in a patient with disseminated *M. tuberculosis*, coronal (A) and sagittal (B) images. The area biopsied after the scan is indicated by the arrowhead.

patients started on antitoxoplasma treatment before the scan, and although this therapy was given for less than 5 days, it is possible that it may have altered FDG and MET uptake. Thus, an earlier scan with no treatment may give entirely different results, e.g., with acute inflammation, high uptake may be seen without treatment; it is therefore possible that patients should be scanned after several days on therapy to improve the discrimination between toxoplasmosis and lymphoma. Patients with progressive multifocal leukoencephalopathy had low uptake of FDG in the region of the lesions, and MET uptake was essentially similar to the contralateral brain. In our experience, a SUV threshold can be set such that those patients with a SUV below 2.5 or less than the contralateral brain should be treated empirically as toxoplasmosis cases, and those with a SUV above 3.9 or 1.5 times greater than the opposite brain tissue could be regarded as lymphoma cases. Between these thresholds, a biopsy should be performed. Failure of treatment response, unfortunately, is common in cerebral toxoplasmosis, and a clinical decision would be made as to whether treatment failures should be biopsied; this decision is made more difficult in patients with a bleeding diathesis. MET does not appear to add to the separation of the two conditions, and indeed in one case, there was divergence between the uptake of MET and FDG in a single area where the patient did have toxoplasmosis. The low uptake of both FDG and MET in progressive multifocal leukoencephalopathy is expected because it is predominantly a demyelinating problem.

The alternative technique that is under investigation is the use of ^{201}Tl scans to assess the grade of cerebral gliomas with higher uptake being found in the more malignant tumors (*37*). Recently Ruiz et al. (*38*) have suggested that ^{201}Tl may be of value in distinguishing between cerebral lymphoma and toxoplasma infection. Lorberboym et al. (*39*) have demonstrated that the retention of thallium is longer in patients with lymphoma than other benign pathologies in the brain. The value of this promising technique has yet to be established, but it is clear that the anatomical resolution will not match PET resolution. Therefore, comparison of uptake with all lesions identified on MRI may be difficult, and the possibility of missing a mixture

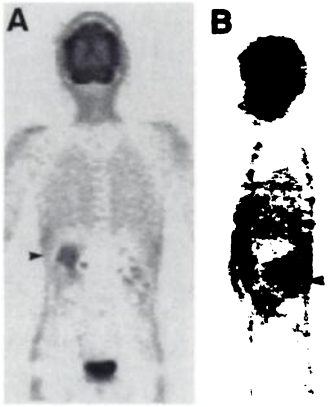

FIGURE 12. FDG uptake in a *Staphylococcus aureus* abscess of the right kidney (indicated by the arrowheads), coronal (A) and sagittal (B) images.

toxoplasma and lymphoma is still present. The radiation dosimetry is also higher with thallium: effective dose equivalent from 80 MBq is 20 mSv, compared with a combined effective dose equivalent for MET and FDG of 9.5 mSv. The advantage of thallium is, of course, that it would be more readily accessible to a larger number of physicians tending patients with AIDS. The advantage of PET is that both the brain and the body can be assessed at the one visit, and our study demonstrates that it should be possible to obtain a scan within a few days of admission. A direct comparison of the methods is needed.

The uptake of FDG in the cortex of the group of patients who had no cognitive dysfunction nor focal cerebral pathology was generally reduced in comparison to the basal ganglia uptake, and this was substantiated by the semiquantitative analysis. It is not possible without quantitative analysis, however, to state whether this finding is due to a global cortical hypometabolism or hypermetabolism in the basal ganglia. All of these patients had CD4 T-lymphocyte counts of less than 200 cells/mm^3 but no overt evidence of dementia. These findings agree with those previously demonstrated by van Gorp et al. (*40*) and Hinkin et al. (*41*). Changes in metabolism are generally more sensitive than changes seen on MR scan and CT (*42*). Quantitative studies would be of use to evaluate the changes with time in HIV-positive individuals and perhaps allow early assessment of the effect of new antiviral therapy regimes on cerebral function.

The use of FDG and MET in the evaluation of three patients with Kaposi's sarcoma of the lung was poor. Although the lesions were visualized, the uptake was low and may well reflect the extra blood-pool activity related to these lesions. None of the skin lesions could be readily identified. The limited number of patients studied does not allow any firm conclusion, and further work needs to be performed in patients with Kaposi's sarcoma in the lung or other organs before the method is abandoned as a possible imaging tool.

The results suggest that FDG-PET can benefit the patient and the clinician in several ways. Potentially, the technique reduces radiation dose and decreases the number of hospital visits or at least the number of scans in patients who are unwell, to direct further investigation. The true cost effectiveness can be assessed by comparison with the other localizing tests but particularly with ^{67}Ga scanning, and this undoubtedly needs to be undertaken. Alternatively, the cost benefit can be assessed on theoretical grounds using a predictive strategy using PET in one assessment arm. The prevalence of causes of focal pathological abnormality in this group may be difficult to assess, especially with the change in prevalence of lymphoma and mycobacterial infections accompanying the new antiviral therapies.

CONCLUSION

This preliminary study has shown that PET enables rapid assessment of the whole body, including the brain, in HIV-positive patients. PET provided accurate and speedy localization of malignant as well as infective disease in patients, allowing biopsy of specific sites to be performed or treatment to be instigated. High FDG uptake visually in infection may provide difficulties in the separation of malignancy from infection in some cases. The technique, if available in a hospital, will allow a scan result, which can be semiquantitative if required, within 2.5 hr. Unlike labeled leukocytes, no complex labeling procedure is required and, unlike gallium, an early result is possible. A direct comparison between gallium and FDG-PET needs to be undertaken to ensure that FDG-PET at least localizes into the same abnormalities as gallium. It is likely, however, that the superior resolution of PET cameras

and the biokinetic distribution of FDG will provide enhanced diagnostic capability. The cost of a PET scan is more than high-dose gallium scanning, but the radiation dose is less and the capability of evaluating the brain at the same imaging session is a potential bonus. The time saved by getting a diagnostic result may be put to more appropriate use for the treatment or further investigation of a patient. The other area that is of potential use in this group is the absolute quantitation of uptake, which could be used in the assessment of response to therapy at an early stage of treatment; this remains to be tested. FDG-PET scanning has a role in the assessment of the HIV-positive patient with a pyrexia of unknown origin, weight loss and suspected cerebral lymphoma and for staging the extent of lymphoma in the body.

REFERENCES

1. Centers for Disease Control. 1993 revised classification system for HIV infection and expanded surveillance case definition for AIDS among adolescents and adults. *Morb Mortal Wkly Rep* 1992;41,RR-17.
2. World Health Organization. Acquired immunodeficiency syndrome (AIDS). 1987 revision of CDC/WHO case definition for AIDS. *Wkly Epidemiol Rec* 1988;63:1–7.
3. Ancelle-Park R. Expanded European AIDS case definition. *Lancet* 1993;341:441.
4. Bitran J, Beckerman C, Weinstein R, Bennet C, Ryo U, Pinsky S. Patterns of gallium-67 scintigraphy in patients with acquired immunodeficiency syndrome and the AIDS related complex. *J Nucl Med* 1987;28:1103–1106.
5. Kramer EL, Sanger JJ, Garay SM, et al. Gallium-67 scans of the chest in patients with acquired immunodeficiency syndrome. *J Nucl Med* 1987;28:1107–1114.
6. Palestro CJ. The current role of gallium imaging in infection. *Semin Nucl Med 1994;24:128–141.*
7. Tatsch K, Knesewitsch, Matuschke A, Wainryb HJ, Goebel F-D, Kirsch CM. Gallium-67 scintigraphy for evaluation of AIDS-related intestinal infections. *Nucl Med Commun* 1990;11:649–655.
8. Woolfenden JM, Carrasquillo JA, Larson SM, et al. Acquired immunodeficiency syndrome. Gallium-67 citrate imaging. *Radiology* 1987;162:383–387.
9. Palestro CJ, Zakheim DS. Gallium-67 abdominal imaging in HIV (+) and HIV (−) patients [Abstract]. *J Nucl Med* 1994;35:174.
10. Strauss LG, Conti PS. The applications of PET in clinical oncology. *J Nucl Med* 1991;32:623–648.
11. Newman J, Francis I, Kaminski M, Wahl R. FDG-PET imaging in lymphoma: correlation with CT. *Radiology* 1994;190:111–116.
12. Alavi JB, Alavi A, Chawluk J, et al. PET in patients with glioma. A predictor of prognosis. *Cancer* 1988;62:1074–1078.
13. DiChiro G, DeLaPlaz RL, Brooks RA, et al. Glucose utilization of cerebral gliomas measured by ^{18}F-fluorodeoxyglucose and PET. *Neurology* 1982;32:1323–1329.
14. Hoffman JM, Waskin HA, Schifter T, et al. FDG-PET in differentiating lymphoma from nonmalignant central nervous system lesions in patients with AIDS. *J Nucl Med* 1993;34:567–575.
15. Ogawa T, Shishido F, Kanno I, et al. Cerebral glioma: evaluation with methionine PET. *Radiology* 1993;186:45–53.
16. Ishii K, Ogawa T, Hatazawa J, et al. High L-methyl-[^{11}C]methionine uptake in brain abscess: a PET study. *J Comput Assist Tomogr* 1993;17:660–661.
17. Bjurling P, Reineck R, Westerberg G, et al. Synthia, a compact radiochemistry system for automated production of radiopharmaceuticals [Abstract]. *Sixth workshop on targetry and automation.* Vancouver 1995.
18. Berridge MS, Cassidy EH, Miraldi F. Carbon-11-acetate and ^{11}C-methionine: improved synthesis and Q.C. *Appl Radiat Isot* 1995;46:173–175.
19. Bergstrom M, Litton J, Eriksson L, Bohm C, Blomquist G. Determination of object contour projections for attenuation correction in cranial positron emission tomography. *J Comput Assist Tomogr* 1982;6:365–372.
20. Hoffman EJ, Huang SC, Phelps ME. Quantitation in positron emission tomography. 1. Effect of object size. *J Comput Assist Tomogr* 1979;3:299–308.
21. Mirales P, Moreno S, Pereztascon M, Cosin J, Diaz MD, Bouza E. Fever of uncertain origin in patients infected with the human immunodeficiency virus. *Clin Infect Dis* 1995;20:872–875.
22. Tuazon CV, Delaney MD, Simon GL, et al. Utility of gallium-67 scintigraphy and bronchial washings in the diagnosis and treatment of *Pneumocystis carinii* pneumonia in patients with the acquired immunodeficiency syndrome. *Am Rev Respir Dis* 1985;132:1087–1092.
23. O'Doherty MJ, Page CJ, Bradbeer CS, et al. The place of lung ^{99m}Tc-DTPA aerosol transfer in the investigation of lung infections in HIV positive patients. *Respir Med* 1989;83:395–401.
24. Rosso J, Guillon JM, Parrot A, et al. Technetium-99m-DTPA aerosol and gallium-67 scanning in pulmonary complications of human immunodeficiency virus infection. *J Nucl Med* 1992;33:81–87.
25. Meikle SR, Bailey DL, Hooper PK, et al. Simultaneous emission and transmission measurements for attenuation correction in whole-body PET. *J Nucl Med* 1995;36: 1680–1688.
26. Barrington SF, Carr R. Staging of Burkitt's lymphoma and response to treatment monitored by PET scanning. *Clin Oncol* 1995;7:334–335.
27. Ichiya Y, Kuwbara Y, Otsuka M, et al. Assessment of response to cancer therapy using fluorine-18-fluorodeoxyglucose and positron emission tomography. *J Nucl Med* 1991;32:1655–1660.
28. Minn HR, Paul R, Ahonen A. Evaluation of treatment response to radiotherapy in head and neck cancer with fluorine-18-fluorodeoxyglucose. *J Nucl Med* 1988;19:1521–1525.
29. Hoekstra OS, Ossenkoppele GJ, Golding R, et al. Early treatment response in malignant lymphoma, as determined by planar fluorine-18-fluorodeoxyglucose scintigraphy. *J Nucl Med* 1993;34:1706–1710.
30. Patz EF, Lowe VJ, Hoffman JM, et al. Focal pulmonary abnormalities: evaluation with ^{18}F-fluorodeoxyglucose PET scanning. *Radiology* 1993;188:487–490.
31. Levy RM, Bredesen DE, Rosenblum ML. Neurological manifestations of the acquired immunodeficiency syndrome (AIDS): experience at UCSF and a review of the literature. *J Neurosurg* 1985;65:475–495.
32. Rosenblum ML, Levy RM, Bredesen DE. Neurosurgical implications of the acquired immunodeficiency syndrome (AIDS). *Clin Neurosurg* 1988;22:700–706.
33. Gray F, Belec L, Keohane C, et al. Zidovudine therapy and HIV encephalitis: a 10-year neuropathological survey. *AIDS* 1994;8:489–493.
34. Whelan MA, Kricheff II, Handler M, et al. Acquired immunodeficiency syndrome: cerebral computed tomographic manifestations. *Radiology* 1993;149:477–484.
35. Rosenfeld SS, Hoffman JM, Coleman RE, Glantz MJ, Hanson MW, Schold SC. Studies of primary central nervous system lymphoma with [^{18}F]fluorodeoxyglucose PET. *J Nucl Med* 1992;33:532–536.
36. Villringer K, Jager H, Dichgans M, et al. Differential-diagnosis of CNS lesions in AIDS patients by FDG PET. *J Comput Assisted Tomogr* 1995;19:532–536.
37. Oriuchi N, Tamura M, Shibazaki T, et al. Clinical evaluation of thallium-201 SPECT in supratentorial gliomas: relationship to histologic grade, prognosis and proliferation activities. *J Nucl Med* 1993;34:2085–2089.
38. Ruiz A, Ganz WI, Post JD, et al. Use of thallium-201 brain SPECT to differentiate cerebral lymphoma from toxoplasma encephalitis in AIDS patients. *Am J Neuroradiol* 1994;15:1885–1894.
39. Lorberboym M, Estok L, Machac J, et al. Rapid differential diagnosis of cerebral toxoplasmosis and primary central nervous system lymphoma by thallium-201 SPECT. *J Nucl Med* 1996;37:1150–1154.
40. van Gorp WG, Mandelkern MA, Gee M, et al. Cerebral metabolic dysfunction in AIDS: findings in a sample with and without dementia. *J Neuropsychiatr* 1992;4:280–287.
41. Hinkin CH, van Gorp WG, Mandelkern MA, et al. Cerebral metabolic change in patients with AIDS: report of a six-month follow-up using PET. *J Neuropsychiatr* 1995;7:180–187.
42. Kim DM, Tien R, Byrum C, Ranga Rama Krishnan K. Imaging in acquired immune deficiency syndrome dementia complex (AIDS dementia complex): a review. *Prog Neuropsychopharmacol Biol Psychiatry* 1996;20:349–370.